Appl. Phys. B 91, 45–48 (2008)
DOI: 10.1007/s00340-008-2956-z

Applied Physics B
Lasers and Optics

J. BERNHARDT[1,✉]
W. LIU[1,2]
S.L. CHIN[1]
R. SAUERBREY[3]

Pressure independence of intensity clamping during filamentation: theory and experiment

[1] Centre d'Optique, Photonique et Laser (COPL) et le Département de Physique, de Génie Physique et d'Optique, Université Laval, Québec, Québec G1V 0A6, Canada
[2] Institute of Modern Optics, Nankai University, Key Laboratory of Opto-electronic Information Science and Technology, Education Ministry of China, Tianjin 300071, P.R. China
[3] Forschungszentrum Dresden-Rossendorf, Bautzner Landstraße 128, 01328 Dresden, Germany

Received: 7 December 2007/Revised version: 25 January 2008
Published online: 28 February 2008 • © Springer-Verlag 2008

ABSTRACT Because of the dynamic equilibrium between Kerr self-focussing and plasma induced defocusing and the inexistence of collisional ionization the critical intensity during femtosecond laser filamentation in air is independent of pressure. An analytical analysis is given which is justified by a direct experimental verification.

PACS 42.65.Jx; 52.38.Hb; 52.70.Kz

1 Introduction

When a laser pulse of high power $P > 10\,\mathrm{GW}$ and ultrashort pulse duration $\tau < 1\,\mathrm{ps}$ and UV, visible, or near IR wavelength propagates in gaseous or transparent dielectric media, light filaments are formed. The laser light is guided in these filaments which consist of weakly ionized matter. In a previous paper [1], we discussed this phenomenon and showed that, as a result of the propagation of a femtosecond Ti:sapphire laser in air, the peak intensity inside a filament is clamped to about $4 \times 10^{13}\,\mathrm{W/cm^2}$ due to the balancing act between Kerr self-focussing and the defocusing by the self-generated plasma inside the filament. Since then, other papers have demonstrated experimentally this universal process in gases [2] and condensed matter [3]. Much work was also performed in the long range propagation of such powerful pulses in air [4, 5]. Because of the possibility of generating a filament in the atmosphere for up to many km in altitude [4] where the atmospheric pressure is significantly reduced, it is natural to ask the same question as to what the clamped intensity would become at high altitude [6–9]. It turns out that the clamped intensity is independent of pressure because the only mechanism that controls this clamping phenomenon is multiphoton or tunnel ionization [10] of the gas molecules which are unimolecular processes. No collisional process could be involved with such a short time scale. This short note gives a physical account of this phenomenon [11].

2 Analytical analysis

The fundamental relation of the balance between Kerr self-focussing and plasma defocusing is the equalization of the nonlinear indices due to the Kerr effect and due to the plasma as given by the following equation,

$$\Delta n_{\mathrm{Kerr}}(\mathrm{neutral}) \approx \Delta n(\mathrm{plasma}) \text{ or} \tag{1}$$

$$n_2 I \approx N_e(I)/2N_{\mathrm{crit}}\,, \tag{2}$$

where Δn is the index change, n_2 the Kerr nonlinear index of refraction, I the intensity, N_e the electron density induced by tunnel ionization of air molecules and N_{crit} the critical plasma density given by

$$N_{\mathrm{crit}} = \varepsilon_0 m\omega^2/e^2, \tag{3}$$

with e, m and ω being the elementary charge, the electron mass and the central frequency of the laser field, respectively. Detailed theoretical work [12] has revealed that the equilibrium between Kerr self-focussing and plasma induced defocusing of the laser light is of a complex dynamic nature. However, the essential physics and the relevant orders of magnitude are governed by (2). In the following we treat laser propagation in air as an example. Essentially, identical arguments apply to any gas or gas mixture. In air the electron density N_e comes from tunnel ionization or multiphoton ionization of both the oxygen and nitrogen molecules through the following rate equation,

$$\begin{aligned}\frac{\mathrm{d}N_e(I)}{\mathrm{d}t} &= R_{\mathrm{N_2}}(I)N_{\mathrm{N_2}} + R_{\mathrm{O_2}}(I)N_{\mathrm{O_2}} \\ &= R_{\mathrm{N_2}}(I)\,0.78N_{\mathrm{air}} + R_{\mathrm{O_2}}(I)\,0.21N_{\mathrm{air}}\,,\end{aligned} \tag{4}$$

where R_A, N_A ($A = \mathrm{N_2}$ or $\mathrm{O_2}$) denote the rate of ionization and the density of molecule A respectively. By integrating this equation, we obtain

$$N_e(I) = N_{\mathrm{air}}\left[0.78\int R_{\mathrm{N_2}}(I)\,\mathrm{d}t + 0.21\int R_{\mathrm{O_2}}(I)\,\mathrm{d}t\right], \tag{5}$$

where the integrals inside the bracket are independent of the air density N_{air}. This approximation is valid as long as the electron density N_e stays well below the neutral air density N_{air} ($N_e \ll N_{\mathrm{air}}$) which is justified for usual experimental condition where N_e has been measured to be in the range of $N_e \approx 10^{14}$–$10^{17}\,\mathrm{cm^{-3}}$ [13–19] which is small compared to $N_{\mathrm{air}} \approx 2.5 \times 10^{19}\,\mathrm{cm^{-3}}$ at atmospheric pressure. The nonlinear index of refraction n_2 is proportional to the air density expressed as

✉ Fax: +1-418-656-2623, E-mail: jens.bernhardt@gmail.com

$$n_2 = \kappa N_{\text{air}} , \tag{6}$$

where κ is a proportionality constant that depends on the detailed electronic structure of the material, but is virtually density independent for gases of atmospheric pressure, and has only a weak density dependence for solids. Putting (5) and (6) into (2), we obtain

$$\kappa N_{\text{air}} I \approx (1/2N_{\text{crit}}) N_{\text{air}} \times \left[0.78 \int R_{\text{N}_2}(I)\,\mathrm{d}t + 0.21 \int R_{\text{O}_2}(I)\,\mathrm{d}t\right]. \tag{7}$$

Eliminating N_{air} from the two sides of (7), we get

$$I \approx (1/2N_{\text{crit}}\kappa)\left[0.78 \int R_{\text{N}_2}(I)\,\mathrm{d}t + 0.21 \int R_{\text{O}_2}(I)\,\mathrm{d}t\right]. \tag{8}$$

The solution of (8) yields the critical intensity $I_{\text{crit}} \approx 4 \times 10^{13}\,\text{W/cm}^2$ for atmospheric air [1]. The ionization rates R are uni-molecular processes and are independent of pressure. Thus, the critical intensity is independent of pressure. The reason for this surprising behaviour lies in the equilibrium between the Kerr effect and ionization as well as the fact that the pulse is so short that no collisional ionization effect is involved in the propagation process. Similar arguments would lead to only a weak density dependence of the critical intensity in solids.

3 Experiment and results

So far, the theory tells us that the critical (clamped) intensity in air or other gases is independent of pressure. It is important that this theoretical understanding be verified by a direct experiment. As a case study, we chose the noble gas helium, which is very "clean". It is mono-atomic and there is no Raman effect nor any complication such as molecular association and fragmentation. Also, the Kerr nonlinearity of helium is two orders of magnitude smaller ($n_2 \sim 10^{-21}\,\text{cm}^2/\text{W}$ [20, 21]) than that of air ($n_2 \sim 10^{-19}\,\text{cm}^2/\text{W}$). Therefore, in helium the critical intensity would be much higher.

In the experiment, 10 Hz, 42 fs pulses (central wavelength: ~ 800 nm) with an energy of 35 mJ were weakly focused ($f = 100$ cm) into a gas chamber filled with pure helium whose pressure could be varied up to one atmosphere. The pulse propagated through helium and created a plasma-filament. The helium fluorescence was collected from the side by imaging the length of the filament onto the entrance slit of a spectrometer (Acton Research, Spectra Pro-500i). The presence of a single filament was verified by observing the fluorescence in the spectrometer's imaging mode by using the zero order of the 1200 grooves/mm grating with the slit fully opened. The spectral resolution of the 1200 grooves/mm grating was about 0.4 nm (slit width: 100 μm) [22]. The spectrometer was equipped with a gated intensified CCD (ICCD, Princeton Instruments Pi-Max 512). The ICCD gate width was set to 20 ns and the detection window was opened with zero delay after the laser–plasma interaction. The spectra were accumulated 20 times. The detector's response was calibrated in the range of 250–800 nm using a tungsten lamp.

As a spectral signature, we can use the atomic line He I 587.56 nm ($1s2p\ ^3P^0$–$1s3d\ ^3D$) [23, 24]. This line is a consequence of tunnel ionization followed by the recombination of He^+ and an electron. Note that this signature is very "clean". In particular, the dynamic range with respect to the 3σ standard deviation of the background noise level is larger than $\sim 10^3$ (20 accumulations, moderate ICCD gain of 125, where the maximum gain is 250). The clean fluorescence is unique to "filament induced plasma spectroscopy" [25, 26], which is another consequence (besides the pressure independence of intensity clamping) of the fact that the filament plasma is generated by tunnel ionization only without the occurrence of inverse Bremsstrahlung and cascade (avalanche) ionization [10].

Since the independence of the critical intensity on pressure (8) is under the approximation $N_e \ll N_{\text{air}}$ of (5), we justify this approximation first in our experiment. We measure the electron density by means of spectroscopy, which has been proven reliable before ([19] and references therein). From the Stark broadening of the He I 587.56 nm line, the maximum electron density is estimated to be about $7 \times 10^{17}\,\text{cm}^{-3}$. This leads to an ionization degree of about 10^{-2}, justifying the above approximation. The critical intensity derived from the ionization curve of He^+ has been measured to be about $7.8 \times 10^{14}\,\text{W/cm}^2$ (to be published). Note that the contribution of He^+ prevails over that of He^{++} in the relevant intensity range [27].

Figure 1 shows the electron density versus pressure curve. The electron densities derived from Stark broadening of the He I 587.56 nm line (see Fig. 2) were measured for different pressures in the range of 50 to 760 Torr. The input power was fixed at ~ 833 GW (42 fs at 35 mJ). The electron density in-

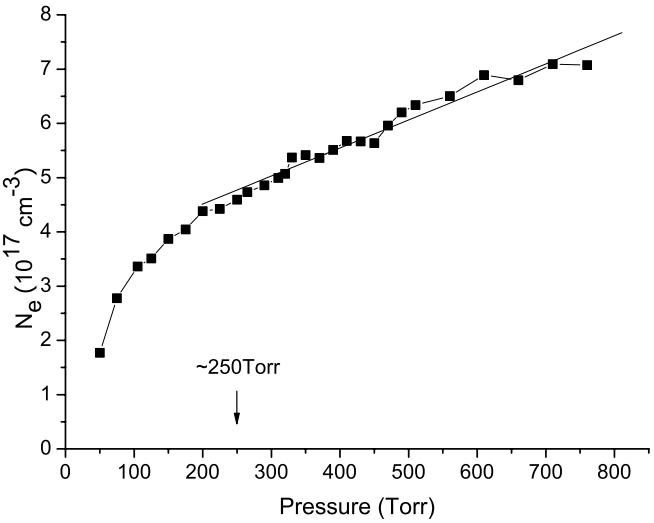

FIGURE 1 Intensity clamping: pressure independence. The data show the electron density derived from Stark broadening of the atomic line He I 587.56 nm versus pressures ranging from 50 to 760 Torr. The pulse duration and energy were fixed at about 42 fs and 35 mJ, respectively. It can be clearly seen that the electron density increases linearly with pressure (linear fit) beyond the critical pressure of about ~ 250 Torr. The consequence of this behaviour is the pressure independence of the critical (clamped) intensity (see text). The critical pressure marks the threshold for Kerr self-focussing. The maximum electron density is about $\sim 7 \times 10^{17}\,\text{cm}^{-3}$, which is well below the depletion limit (ionization degree: $\sim 10^{-2}$)

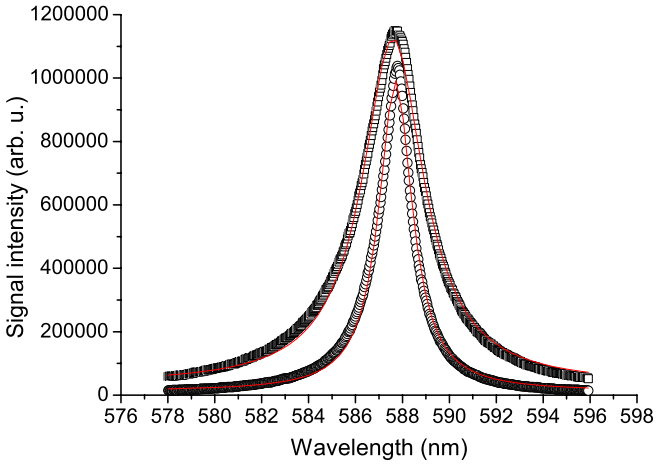

FIGURE 2 He I 587.56 nm spectral lines. The data show the Stark broadened He I 587.56 nm lines recorded at pressures of ∼150 Torr (*black circles*) and ∼ 760 Torr (*black squares*), respectively, fitted by Lorentzian profiles (*red curves*). The pulse duration and energy are the same as in Fig. 1. The good fitting also indicates the absence of self-absorption

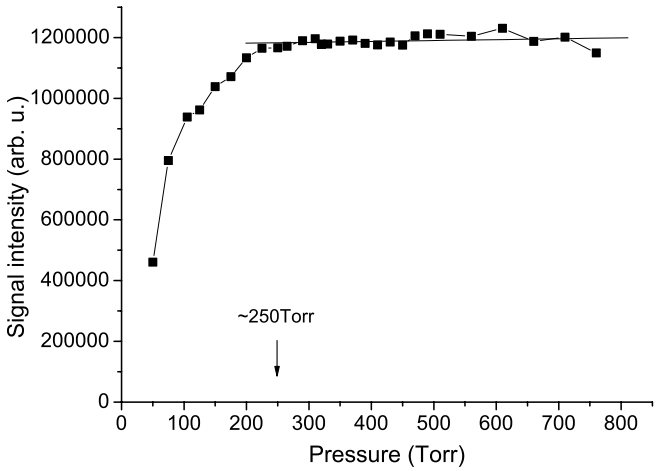

FIGURE 3 Filament volume: pressure independence. The data show the peak intensity of the atomic line He I 587.56 nm versus pressures ranging from 50 to 760 Torr. The pulse duration and energy are the same as in Fig. 1. The peak intensity increases with increasing pressure until the slope tends towards a constant at a critical pressure of about ∼250 Torr. The stable region beyond ∼ 250 Torr (linear fit) indicates intensity clamping (see text). As a consequence, the filament volume stays constant

creases linearly with pressure (Fig. 1, linear fit) beyond a (critical) pressure of about ∼ 250 Torr. It is important to note that there is no depletion of neutrals in the ionization zone (ionization degree: 10^{-2}). The linear behaviour beyond 250 Torr indicates intensity clamping which is expected from (5) adapted to He gas:

$$N_e^{\mathrm{He}}(I) = N_{\mathrm{He}} \int R_{\mathrm{He}}(I)\,\mathrm{d}t\,, \tag{9}$$

where N_{He} and R_{He} are the corresponding values for helium. Equation (9) shows that the electron density scales linearly with pressure if the integral is independent of pressure. Since the integral is a function of the intensity (I), it means that the intensity should be constant as the pressure changes. To recap the experimental observation, at the beginning at low pressures, the critical power for self-focussing is still too high and only linear geometrical focusing gives rise to the fluorescence. At higher pressures starting at around 250 Torr, the critical power decreases to a value equal to the input power. Self-focussing and filamentation sets in at this pressure. From this pressure on, the intensity no longer changes with pressure.

Figure 3 shows the peak intensity of the atomic line He I 587.56 nm as a function of pressure in the range of 50–760 Torr. The pulse duration and energy are the same as in Fig. 1. The peak intensity increases with increasing pressure until the slope tends towards a constant at a critical pressure of about ∼ 250 Torr. The stable region beyond ∼ 250 Torr (Fig. 3, linear fit) indicates intensity clamping (see above). This implies that the filament volume stays constant.

Note that we are still in a power regime where relativistic effects are negligible. In fact, the critical power for Kerr self-focussing is given by Marburger's equation [28],

$$P_{\mathrm{crit}}^{\mathrm{Kerr}} = \frac{3.77\lambda^2}{8\pi n_0 n_2}\,, \tag{10}$$

where λ is the central laser wavelength and n_0 the linear index of refraction. However, relativistic self-focussing sets in at a much higher critical power, which is given by [29],

$$P_{\mathrm{crit}}^{\mathrm{rel}} \sim 16.2\frac{N_{\mathrm{crit}}}{N_e}\,\mathrm{GW}\,. \tag{11}$$

Inserting the maximum electron density of $\sim 7\times10^{17}\,\mathrm{cm}^{-3}$ yields $P_{\mathrm{crit}}^{\mathrm{rel}} \sim 40$ TW. This is about two orders of magnitude higher than $P_{\mathrm{crit}}^{\mathrm{Kerr}} \sim 10^2$ GW (putting $n_2 \sim 3.6\times10^{-21}\,\mathrm{cm}^2/\mathrm{W}$ [20, 21] in (10)). Therefore, relativistic self-focussing is negligible.

4 Conclusion

In conclusion, we have shown both theoretically and experimentally that the critical intensity in air or other gases is independent of pressure. A consequence of this phenomenon in vertical atmospheric propagation is that the filament size (diameter) will become larger and larger as the altitude increases because of the following reason. Since the critical power for self-focussing P_{c} is inversely proportional to n_2 (10) and since n_2 is proportional to the air density (6), the critical power for self-focussing increases as the pressure at higher altitude decreases. Hence, to obtain self-focussing at higher altitude, the input peak power of the pulse has to increase. However, since the intensity is clamped at the value at sea level, the higher peak power of the pulse has to be contained inside a region with a larger diameter than that at sea level.

ACKNOWLEDGEMENTS The authors thank A. Mysyrowicz and B. Prade for very fruitful discussion. RS acknowledges the support by the German Research Foundation (DFG) and the Teramobile Research group. WL acknowledges the support of NSFC, NCET and the Chinese National Major Basic Research Development Program, while SLC acknowledges the support of NSERC, Canada Research Chairs Program, DRDC-Valcartier and the Alexander von Humboldt Foundation.

REFERENCES

1 J. Kasparian, R. Sauerbrey, S.L. Chin, Appl. Phys. B **71**, 877 (2000)
2 A. Becker, N. Aközbek, K. Vijayalakshmi, E. Oral, C.M. Bowden, S.L. Chin, Appl. Phys. B **73**, 287 (2001)

3 W. Liu, S. Petit, A. Becker, N. Aközbek, C.M. Bowden, S.L. Chin, Opt. Commun. **202**, 189 (2002)
4 M. Rodriguez, R. Bourayou, G. Méjean, J. Kasparian, J. Yu, E. Salmon, A. Scholz, B. Stecklum, J. Eislöffel, U. Laux, A.P. Hatzes, R. Sauerbrey, L. Wöste, J.-P. Wolf, Phys. Rev. E **69**, 036 607 (2004)
5 S.A. Hosseini, Q. Luo, B. Ferland, W. Liu, S.L. Chin, O.G. Kosareva, N.A. Panov, N. Aközbek, V.P. Kandidov, Phys. Rev. A **70**, 033 802 (2004)
6 P. Sprangle, J.R. Peñano, B. Hafizi, Phys. Rev. E **66**, 046 418 (2002)
7 E. Arévalo, Phys. Rev. E **74**, 016 602 (2006)
8 G. Méchain, G. Méjean, R. Ackermann, P. Rohwetter, Y.-B. André, J. Kasparian, B. Prade, K. Stelmaszczyk, J. Yu, E. Salmon, W. Winn, L.A. Schlie, A. Mysyrowicz, R. Sauerbrey, L. Wöste, J.-P. Wolf, Appl. Phys. B **80**, 785 (2005)
9 L. Bergé, S. Skupin, R. Nuter, J. Kasparian, J.-P. Wolf, Rep. Prog. Phys. **70**, 1633 (2007) and references therein
10 S.L. Chin, From Multiphoton to Tunnel Ionization, in *Advances in Multiphoton Processes and Spectroscopy*, ed. by S.H. Lin, A.A. Villaeys, Y. Fujimura (World Scientific, Singapore, 2004), vol. 16, pp. 249–272
11 B. Prade, Study of filamentation in gases as a function of pressure, in Joint ICONO/LAT Symposium, Femtosecond Laser Pulse Filamentation: Phenomena and Applications, St. Petersburg, Russia, May 11–15, Invited Talk (2005)
12 M. Kolesik, J.V. Moloney, Phys. Rev. E **70**, 036 604 (2004) and references therein
13 A. Talebpour, A. Abdel-Fattah, S.L. Chin, Opt. Commun. **183**, 479 (2000)
14 H. Schillinger, R. Sauerbrey, Appl. Phys. B **68**, 753 (1999)
15 S. Tzortzakis, B. Prade, M. Franco, A. Mysyrowicz, Opt. Commun. **181**, 123 (2000)
16 B. La Fontaine, F. Vidal, Z. Jiang, C.Y. Chien, D. Comtois, A. Desparois, T.W. Johnston, J.-C. Kieffer, H. Pépin, H.P. Mercure, Phys. Plasmas **6**, 1615 (1999)
17 C.Y. Chien, B. La Fontaine, A. Desparois, Z. Jiang, T.W. Johnston, J.C. Kieffer, H. Pépin, F. Vidal, H.P. Mercure, Opt. Lett. **25**, 578 (2000)
18 F. Théberge, W. Liu, P.T. Simard, A. Becker, S.L. Chin, Phys. Rev. E **74**, 036 406 (2006)
19 J. Bernhardt, W. Liu, F. Théberge, H.L. Xu, J.-F. Daigle, M. Châteauneuf, J. Dubois, S.L. Chin, Opt. Commun. **281**, 1268 (2008)
20 E.T.J. Nibbering, G. Grillon, M.A. Franco, B.S. Prade, A. Mysyrowicz, J. Opt. Soc. Am. B **14**, 650 (1997)
21 J. Bernhardt, P.T. Simard, W. Liu, H.L. Xu, F. Théberge, A. Azarm, J.F. Daigle, S.L. Chin, Opt. Commun. (2008), doi:10.1016/j.optcom.2007.12.001
22 H.L. Xu, J. Bernhardt, P. Mathieu, G. Roy, S.L. Chin, J. Appl. Phys. **101**, 033 124 (2007)
23 NIST, http://physics.nist.gov/PhysRefData/ASD/index.html (2007)
24 V. Milosavljević, S. Djeniže, Astron. Astrophys. **393**, 721 (2002)
25 A. Talebpour, M. Abdel-Fattah, A.D. Bandrauk, S.L. Chin, Laser Phys. **11**, 68 (2001)
26 J.F. Gravel, Q. Luo, D. Boudreau, X.P. Tang, S.L. Chin, Anal. Chem. **76**, 4799 (2004)
27 B. Walker, B. Sheehy, L.F. Dimauro, P. Agostini, K.J. Schafer, K.C. Kulander, Phys. Rev. Lett. **73**, 1227 (1994)
28 J.H. Marburger, Prog. Quantum. Electron. **4**, 35 (1975)
29 G.Z. Sun, E. Ott, Y.C. Lee, P. Guzdar, Phys. Fluids **30**, 526 (1987)